UNIVERSITA' DEGLI STUDI DI GENOVA

DOTTORATO DI RICERCA XXXI CICLO

CORSO DI MEDICINA TRASLAZIONALE IN ONCOLOGIA ED EMATOLOGIA

CURRICULUM EMATOLOGIA TRASLAZIONALE

METABOLIC STARVATION TRIGGERED BY L-ASPARAGINASE SENSITIZES MULTIPLE MYELOMA CELLS TO PROTEASOME INHIBITORS BY INDUCING DNA DAMAGE ACCUMULATION

Dott.ssa Paola Minetto

Medico Chirurgo – Specialista in Ematologia

Tutor

Prof. Michele Cea

Anno Accademico

2018/2019

1. INTRODUCTION

Multiple Myeloma (MM) is a malignant proliferation of clonal bone marrow (BM) plasma cells (PCs) in association with monoclonal protein.[1] Despite the dramatic improvements in MM treatment achieved in the last decade, it is still an incurable disease. A better knowledge of the biological mechanisms involved in disease occurrence and progression has led to the development of several new, innovative, drugs that significantly improved patients outcome and renewed the therapeutic approach to the disease in the last years. However, resistance develops with a 40% survival at five-years.[2-6] Moreover, despite the improvement of patient risk-stratification systems at diagnosis, treatment outcome is often unpredictable due to the high degree of genomic heterogeneity and genomic instability which characterize the disease. In this view, novel therapeutic strategies capable to overcome disease heterogeneity and improve patient outcome are strongly needed.[7-8]

A fundamental feature of all cancers is the metabolic reprogramming to promote growth, survival, proliferation, and long-term maintenance. The common feature of this altered metabolism is increased glucose uptake and fermentation of glucose to lactate, the so called “Warburg Effect”.[9-12] Moreover, the non essential amino acid Glutamine complements glucose to meet cancer cells metabolic demands. In particular, some human tumors exhibit a high requirement for Gln for anabolic and metabolic processes, a condition that has been defined “Gln-addiction” leading to the investigation of such Gln-dependence as therapeutic target in human cancers.[13-16]

Beside its role of carbon and nitrogen source for macromolecules synthesis, the metabolism of this non-essential amino acid support tumor growth by inducing essential amino acids uptake and activation of mTORC1 signaling pathways, which acts as regulator for protein translation and autophagy.[14-17] Moreover, Gln maintains mitochondrial membrane potential and prevents oxidative damage driving Glutathione (GSH) and NADPH synthesis.[18]

In the recent years the importance of Gln metabolism as therapeutic target began to be explored and emerging data suggest that inhibition of glutamine metabolism with small molecules results in an energetic crisis leading to cellular death.[19-21] Emerging data suggest efficacy of Gln-deprivation also in MM cells which are unable to synthesize adequate amounts of Gln and, therefore, result highly sensitive to Gln-transporters blockade or glutaminase inhibition.[22-24]

Several approaches are reported to achieve Glu-depletion including: uptake inhibition (Gln-transporters inhibitors), metabolism targeting (Glutaminase inhibitors) or serum depletion exploiting the glutaminase-activity of L-asparaginase drug (L-ASP). L-ASP is a bacterial-derived enzyme that induces serum aminoacidic deprivation by catalyzing the hydrolysis of asparagine in aspartic acid and ammonium and glutamine in glutamic acid and ammonium.[24-29] Among the above mentioned strategies to obtain Gln-deprivation, L-ASP is already available in clinic as it represents a cornerstone for acute lymphoblastic leukemia (ALL) and some aggressive lymphomas treatment.

Based on these observations, we aim to explore the therapeutic relevance of Asparaginase-induced Gln depletion alone and in combination with currently used

anti-MM drugs. Moreover we will analyze biological mechanisms supporting the effectiveness of the identified therapeutic strategies.

2. MATHERIALS AND METHODS

2.1 Cell lines, primary cells and reagents

The HMCLs MM.1S, LP1, RPMI-8226, H929, MOLP8, U266 were provided by collaborators or purchased from ATCC (Manassas, Virginia) or DSMZ (Braunschweig, Germany).

HMCLs were maintained in RPMI 8226 medium containing 10% fetal bovine serum (FBS), 2 g/L glucose, 2 mM L-glutamine (GIBCO, Life Technologies, Carlsbad, CA). Medium was additioned with 50 U/mL penicillin/streptomycin and L-glutamine to obtain a final L-glutamine concentration of 4 mM (GIBCO, Life Technologies, Carlsbad, CA).

HEK-293T cell line was purchased from ATCC and cultured in DMEM containing 10% FBS (GIBCO, Life Technologies, Carlsbad, CA), 4mM glutamine, 50 U/ml penicillin, and 50 U/ml streptomycin (GIBCO, Life Technologies, Carlsbad, CA).

To perform experiments in conditions of amino acid deprivation cells were cultured in 10% FBS MEM medium (Sigma-Aldrich) supplemented with penicillin/streptomycin.

Primary CD138+ MM cells were obtained from BM aspirate of newly diagnosed MM patients with high disease burden. Mononuclear cells were isolated by Ficoll-Hypaque gradient and processed by MiniMacs high-gradient magnetic separation column

(Miltenyi Biotec, Bergisch-Gladbach, Germany) to obtain highly purified CD138+ cells. Cells were used immediately for viability assays in RPMI 8226 medium containing 4 mM L-glutamine and 5ng/mL IL-6 to preserve primary CD138+ cells viability.

Human bone marrow stromal cells (BMSC) were isolated from bone marrow aspirates of MM patients. Mononuclear cells were collected by gradient centrifugation and plated in growth medium containing DMEM high glucose 20% FBS and 4Mm L-glutamine. The non-adherent cells were removed after 5 days and the adherent cells cultured for further use.

Erwinia Chrysantemi-derived L-ASP was gently provided by Jazz Pharmaceuticals. Escherichia Coli-derived L-ASP was purchased by Sigma Aldrich (#3809). Carfilzomib was purchased from Selleckchem (#S2853).

2.2 Cell viability and apoptosis assays

For citotoxicity assays, cells viability was assessed by colorimetric method, directly adding an all in one solution of tetrazolium compound inner salt (MTS) and an electron coupling reagent to culture plates (Cell Titer 96® Aqueous, Promega Corporation, Madison, WI, USA). After an incubation time from 30'to 4 hours, absorbance was recorded at 490nm with a 96-well plate reader.

Apoptosis was evaluated by flow cytometric analysis following Annexin V–FITC (BD Bioscences, 556419) and Propidium (PI) (BD Bioscences, 51-6621E) staining, according to manufacturer's instructions. The percentage of cells undergoing apoptosis was

defined as the sum of early apoptotic (annexin V+PI−) and late apoptotic (annexin V+PI+) cells.

Combination drugs screening with L-ASP plus PIs bortezomib and carfilzomib was investigated with an isobologram analysis (CalcuSyn software program, version 2, Biosoft).

2.3 Cell cycle and mitochondrial potential membrane analysis

Cell-cycle profiles were obtained by staining cells with propidium iodide (PI; 50 μg/ml) in hypotonic lysis solution (0.1% (w/v) sodium citrate, 0.1% (v/v) Triton X-100) and incubating at 4°C for 24hours before analysis by flow cytometry.

Mitochondrial potential membrane was measured by flow cytometric analysis after a 15' incubation with 50 nM tetramethylrhodamine ethyl ester (TMRE).

2.4 Intracellular NAD+ measurement

To evaluate the content of intracellular NAD, cells were plated at a density of 10^6 cells/well in 12-well plates and treated with different drugs. After 24 hrs of drug exposure, controls and treated cells were lysed in 0.05 ml of 0.6 M PCA at 4°C. Cell extracts were centrifuged for 3 min at 16, 000 x g, the supernatants were collected and an aliquot was diluted 20-fold in 100 mM sodium phosphate buffer, pH 8.0, for determination of NAD+ content, as described. NAD+ values were normalized to protein concentrations, determined by Bradford assay.[30]

2.5 Lentiviral transduction

pLV control and pLV *c-MYC* over-espressing lentiviral vectors were purchased from Vector Builder (Vector Builder Inc., Santa Clara, USA). For lentiviral transduction, 1×10^6 293T cells were plated on 60 mm Petri dishes and allowed to adhere for 24 h. Thereafter, cells were transfected with 1µg of lentiviral plasmidic DNA and 700ng of each of three packaging vectors (pRP CMV VSVG; pRP CMV gag:pol RRE; pRP CMV RSV Rev), using TransIT-293 (Mirus Bio, Madison, WI) according to the manufacturer's instructions. 48 and 72h after transfection, the supernatant containing lentiviral particles was harvested, filtered with a 0.45-µm-diameter filter, and used to infect MM cells. MM cells were spinoculated at 750g for 45 min in presence of 8 µg ml−1 polybrene, (Santa Cruz Biotechnologies, CA), incubated with viral supernatant for 8 h and left overnight in normal culturing medium. The day after, a second cycle of infection was performed. Successfully infected cells were selected using a suitable concentration of puromycin (0,5-2 µg ml−1). 48 and 72 h after selection, the transduction efficiency was approximated by counting the proportion of cells expressing the fluorescent protein (GFP) using a fluorescence microscope (Nikon Eclipse 80i, Nikon, Melville, NY); and the c-*MYC* over expression was validated by protein level with WB analysis. Functional studies were performed as described below.

2.6 Western blot

Whole-cell lysates were prepared as previously described. 31 Protein concentrations were determined by Bradford assay (Bio-Rad, CA), and equivalent amounts (40-50µg) were subjected to SDS-PAGE, transferred to PVDF membranes immunoblotted with following antibodies: anti-GAPDH (#5174, CellSignaling Technology) -γ tubulin (#MA1-850, ThermoFischer Scientific), -PARP1 (#9532, CellSignaling Technology), -Caspase3 (#9662, Cell Signaling Technology), -c-Myc (#9402, Cell Signaling Technology), CDK4 (#12790 Cell Signaling Technology) – CDK6 (#3136 Cell Signaling Technology) – p21 (#2947 Cell Signaling Technology) – p27 (#3686 Cell Signaling Technology) - Non-phospho-4E-BP1 (Thr46) (#4923, Cell SignalingTechnology), peIF2alpha (#3398 Cell Signaling Technology) eIF2alpha (#5324, Cell Signaling Technology), Phospho-p70 S6 Kinase (Thr389) (#9206,Cell Signaling Technology), phospho-Histone H2A.X (Ser139) (#05-636, Millipore), -RAD51 (#sc-8349, Santa Cruz Biotechnology) – ATF4 (#11815 Cell Signaling Technology) - CHOP (#2895 Cell Signaling Technology) – pAMPK (PA5-17831 Thermo Scientific)– IRF4 (#4964 Cell Signaling Technology).

Band intensities were quantified by Quantity One SW software (Bio-Rad Laboratories, Inc) using standard ECL Western Blotting Detection Reagents (Thermo Fisher Scientific, IL). Densitometric analysis of western blots was carried out using Image J software version 1.48 (National Institute of Health).

2.7 Oxidative stress

To confirm the involvement of ROS in drug-induced apoptosis, HMCLs were treated with L-ASP, PI or combination in presence or absence of 10 mM N-acetylcysteine (NAC). Percentage of cell death was assesses by cytofluorimetric analysis after AV/PI staining.

2.8 Immunofluorescence

DNA damage was detected by confocal microscopy as previously described.[31] The anti-γH2AX antibody was from Millipore (Ser139, clone JBW301) and the secondary Alexa Fluor 488–conjugated antibody was from Jackson Immuno Research. Q-Nuclear was used to counterstain nuclei. The slides were then mounted with ProLong Gold Antifade reagent (Life Technologies Carlsbad, CA), and images were taken using a Leica TCS SP confocal laser scanning microscope (Leica Microsystems, Wetzlar, Germany), equipped with 476, 488, 543 and 633 excitation lines with a 60 x Plan Apo oil objective.

2.9 Nucleofection

RPMI 8226 cells were transfected by using the 4D-Nucleofector™ System (Lonza), according to manufacturer's instruction. pCMV3-empty vector and pCMV3-PARP1-overespressing plasmids was purchased from Sino Biological (Wayne, PA, USA). For each nucleofection, 2 x 10^6 cells were pulsed with the DN-100 program, using Amaxa SF Cell line 4-D Nucleofector X KitL (Lonza). In this procedure, plasmidic DNA was used

at the final concentrations of 500 nM. After 24h from nucleofection, cells were cultured and then treated for further experiments.

3. RESULTS

3.1 L-asparaginase treatment significantly impacts MM cell viability by inducing metabolic "shutdown"

Recent data indicate that tumor cells, including MM, exhibit a "metabolic addctition" that could be therapeutically exploited. 32-34 We exploit the amino acidic-deprivation induced by L-ASP to target MM cells Gln-addiction. Since L-ASP from *E. Chrysantemi* exerts a 10-folder higher glutaminase activity in comparison with Escherichia Coli-derived formulation, we first tested the anti-MM activity of Erwinia Chrysanthemi-derived L-ASP on a large cohort of HMCLs harboring different genetic background. As shown in **Figure 1A**, a significant dose- and time-dependent decrease of MM cells viability was observed, with 50% inhibitory concentration (IC50) values that ranged from 0,03 U/mL to 0.25 U/mL at 48h. To support specificity of this compound, a reference compound with the same reported mechanism of action was also tested; remarkably, the anti-MM activity of E. Coli- derived L-ASP on MM1S and LP1 cells was weaker as compared to Erwinia Chrysanthemi-derived L-ASP (**Figure 1B**). Next, we tested the anti-tumor activity of L-ASP on primary MM cells from both newly-diagnosed as well as relapsed patients. Importantly, such treatment yielded similar results in a time- and dose-dependent manner (data not shown), irrespectively from disease-status derived cells.

A

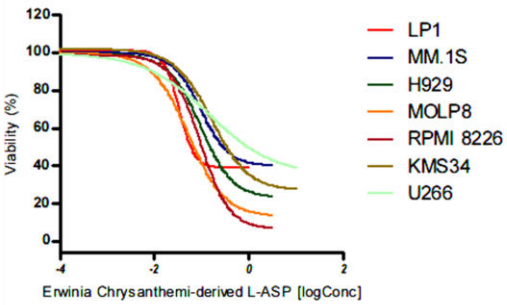

IC_{50}

	LP1	MOLP8	RPMI 8226	H929	MM.1S	KMS34	U266
IC_{50}	0,03327	0,05298	0,09294	0,09425	0,09584	0,1637	0,2471
cMYC	9.9	n.a	10.3	3.1	3.4	19.7	absent
KRAS	wt	MUT	MUT	wt	MUT	n.a	wt
p53	MUT	wt	MUT	wt	wt	MUT	MUT
karyotype	(4;14)	(11;14)	(16;2) (8;22)	(4;14)	(14;16) (8;14)	(4;14)	(11;14)

B

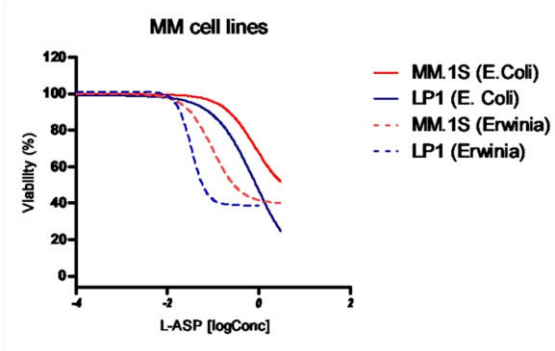

HMCL	E. Coli L-ASP IC_{50} [U/mL]	Erwinia L-ASP IC_{50} [U/mL]
MM.1S	0,8127	0,09584
LP1	0,7933	0,03327

Figure 1. *Erwinia Chrysanthemi* derived L-ASP shows potent anti-MM activity. (**A**) A panel of HMCLs were treated with increasing doses *of Erwinia Chrysanthemi* -derived L-ASP (from 0.01 U/mL to 3 U/mL) in a 96 wells plate and then viability was assessed by a MTS-based assay at 48 h. On the right IC_{50} values of MM tested cell lines is shown, together with detailed description of genetic background. (**B**) MM.1S and LP1 cell lines were tested with E. Chrysantemi L-ASP in parallel with E. Coli L-ASP. Viability was assessed following 48h of treatment by MTS-based assay. Data represent the mean values ± SD and represent a minimum of triplicates.

Importantly, although diminished metabolic activity after drug treatment at 24 hours, MM cells did not enhance their apoptotic rate as determined by Annexin V/Propidium Iodide flow cytometric analysis (data not shown). These data prompted us to hypothesize that MTS assay, by detecting metabolic cells status, overestimated L-ASP anti-MM activity. Indeed, drug-exposure increased PI positive cells (death cells) only in RPMI 8226, whilst mortality rate of almost all tested cells was not measurable. The contribution of each amino-acidic depletion (L-Asn and L-Gln) was next investigated.

Importantly, while single L-Asn withdrawal did not affect MM cells viability at all, the double amino-acidic deprivation as well as Gln-deletion fully summarized the anti-MM activity triggered by L-ASP treatment (**Figure 2A**). We aimed to demonstrate that L-ASP induces a "metabolic shutdown" by analyzing cell cycle phases of MM-treated cells. As shown in **Figure 2B**, a G0/G1 phase arrest was observed early after 24h of treatment. Mechanistically these events were triggered by cMYC downregulation which in turn, by inducing cyclin (CDK4 and CDK6) downregulation and p21 activation, impaired cell cycle progression. As a result, U266 cell line, which does not express c-MYC, were only minimally sensitive to L-ASP with no differences on cell cycle phases between treated and untreated cells. Overall these data supported crucial role played by this oncogene on L-ASP observed anti-MM activity. To confirm these data, a proteomic analysis was also performed. As shown in **Figure 2D**, L-ASP treatment resulted in a massive protein synthesis blockade as suggested by increased non-phospho 4EBP1 and decreased pP70S6K at 48 h which is mediated by ATF4 and CHOP upregulation.

Thus our data show the preclinical activity of L-ASP against both primary cells and MM cell lines.

A

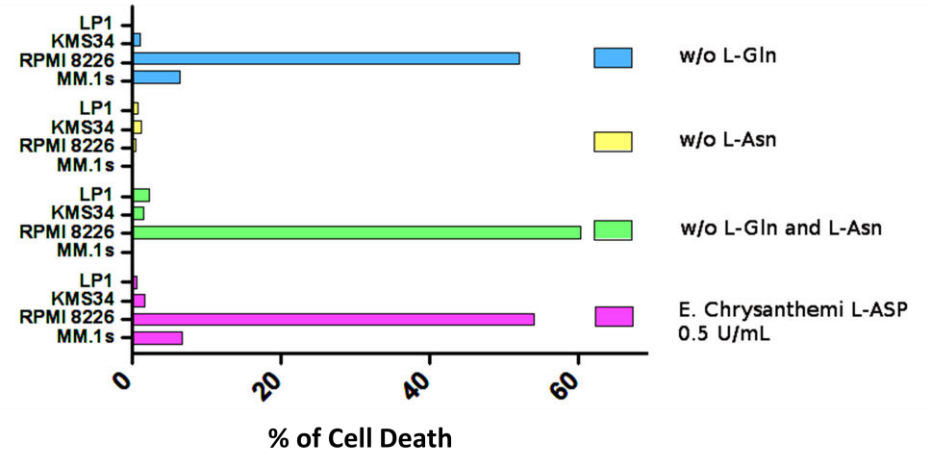
LP1
KMS34
RPMI 8226
MM.1s
w/o L-Gln
w/o L-Asn
w/o L-Gln and L-Asn
E. Chrysanthemi L-ASP
0.5 U/mL
0
20
40
60
% of Cell Death

B

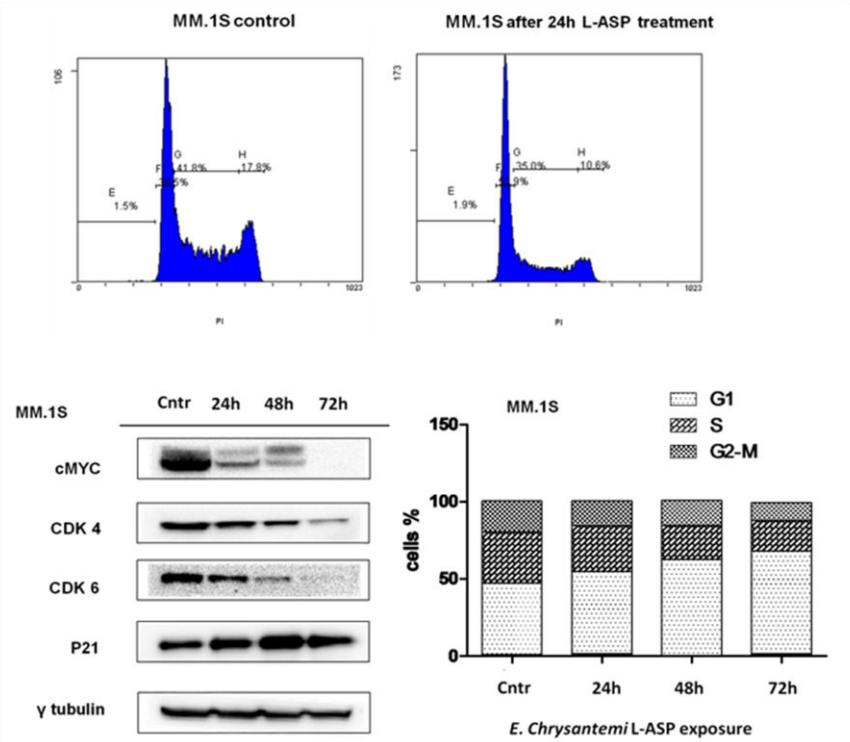
MM.1S control
MM.1S after 24h L-ASP treatment
MM.1S
Cntr
24h
48h
72h
cMYC
CDK 4
CDK 6
P21
γ tubulin
MM.1S
G1
S
G2-M
cells %
150
100
50
0
Cntr
24h
48h
72h
E. Chrysantemi L-ASP exposure

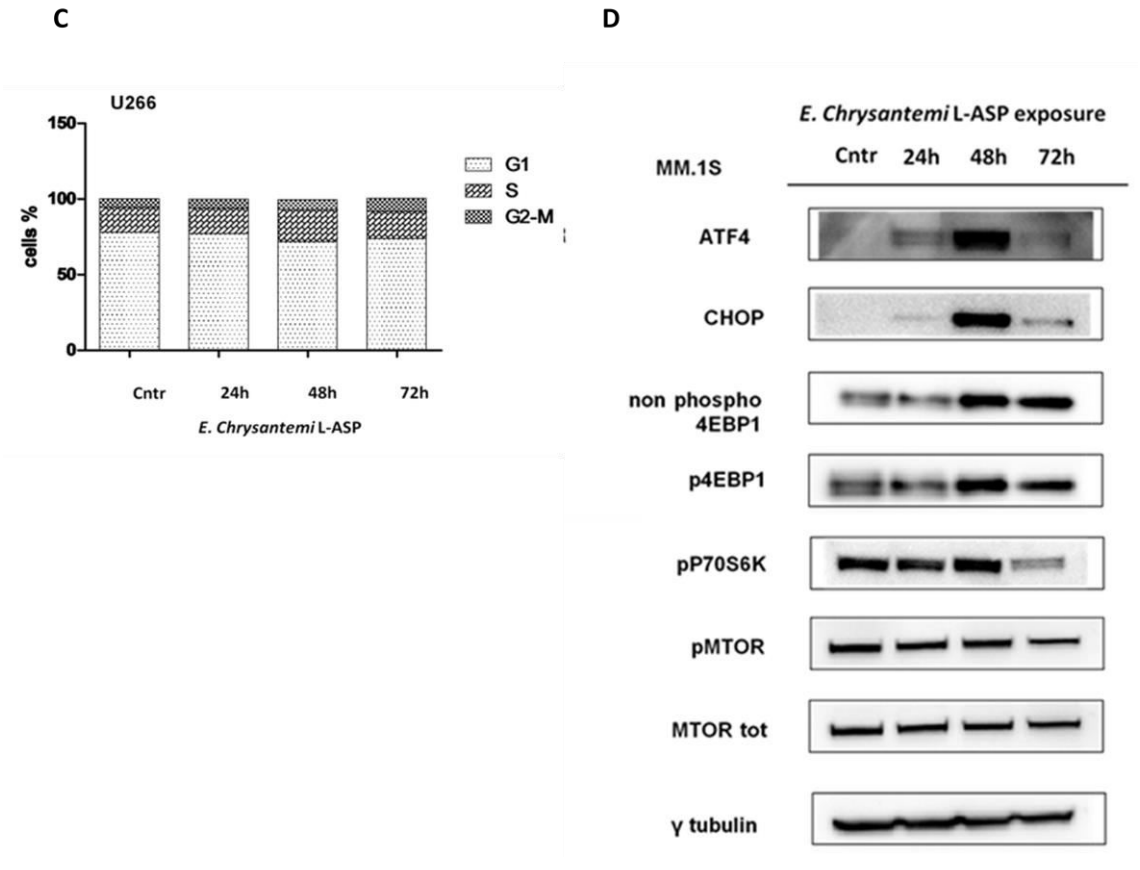

Figure 2. c-MYC plays a crucial role in anti-MM activity of ErwiniaChrysanthemi derived L-ASP. (A) Cell death, measured by FACS analysis of PI stained cells, in different amino-acidic deprivation conditions or after 48 h of *E.Chrysantemi*-derived L-ASP treatment [0.5 U/mL]. **(B)** L-ASP treatment induces a G0/G1 phase arrest after 24 h treatment as well as c-MYC and cyclins downregulation, as depicted in western blot. **(C)** U266 cell lines are resistant to L-ASP-induced cell cycle arrest. **(D)** L-ASP treatment [0.5 U/mL] induces a protein synthesis blockade as shown in western blot analysis of drug-treated MM1S cells at different time exposure.

3.2 Targeting metabolism and proteasome activity triggers synergistic anti-MM activity and results independent from c-MYC downregulation

As reported, targeting metabolic vulnerabilities could exert synergistic anti-tumor activity with established therapies.34-36 We therefore investigated the combinatory effects between L-ASP and drugs currently used for MM treatment, such as the proteasome inhibitors (PIs). In particular, we explored the impact of L-ASP treatment on MM cells sensitivity to both carfilzomib (KAR) and bortezomib (BZ). On the basis of our preliminary data, we selected concentrations of L-ASP and carfilzomib with only modest single agent MM cell citotoxicity in order to assess their combined citotoxicity. Enhanced citotoxicity of the combination treatment in comparison with either agent alone was observed in all MM cell lines (**Figure 3A**); isobologram and combination index analysis revealed strong synergism of the combination as compare to single agents, with a combination index (CI) <1.0 at all tested doses (data not shown). Similarly, potent synergistic activity was observed also on primary tumor cells collected from patients (both NDMM and RRMM), with a CI <1.0 with all tested doses. On the contrary, in healthy PBMCs, these drugs were not only poorly active, but they also failed to show any cooperation. Thus carfilzomib's activity is not potentiated by L-ASP in PBMCs, likely due to their lower proteasome activity,37 suggesting therefore a favorable therapeutic index for such combination. We next examined the molecular mechanism whereby co-treatment triggers synergistic anti-MM cytotoxicity. These studies were performed at 24 hours to reduce the confounding effects of cell death induction at later time points. 38 Combination produced changes in MM cells that are

typically observed during apoptosis, including an increase in the percentage of Annexin-V+/PI- (early apoptotic) and Annexin-V+/P+ (late apoptotic) cells (**Figure 3A**); increased proteolytic cleavage of caspase-3 and PARP-1 in WB analysis (**Figure 3B**). To formally assess the role of caspase activity in MM cell death in response to the stimuli under investigation, we made use of the pan-caspase inhibitor zVAD-fmk. Since the latter strongly reduced cell death in response to L-ASP and KAR combination, we concluded that these compounds kill MM cells via caspase-mediated apoptosis.

To gain insights into specific role played by each amino-acid depletion in the observed synergism, we kept PIs-treated MM cells in different culture medium conditions. Asn depletion alone did not enhance the anti-MM activity of PIs; by contrast, a significant increase of tumor cells toxicity was observed when Gln-starved cells were treated with increased doses of PIs.

Based on the prominent role of the Bone Marrow microenvironment in the progression of MM, and in development of drug-resistance,[39,40] we characterized the effect of the BM milieu on MM sensitivity to this combination. We treated tumor cells in IL-6 (10 ng/mL) or IGF-1 (100 ng/mL). As expected, IL-6 or IGF-1 all protected tumor cells from spontaneous apoptosis but, importantly, co-treatment preserved its efficacy in this context. Thus, compared to spontaneous apoptosis of MM cells, co-treatment increased cell death in MM cells cultured alone but preserved its activity in the presence of BM milieu.

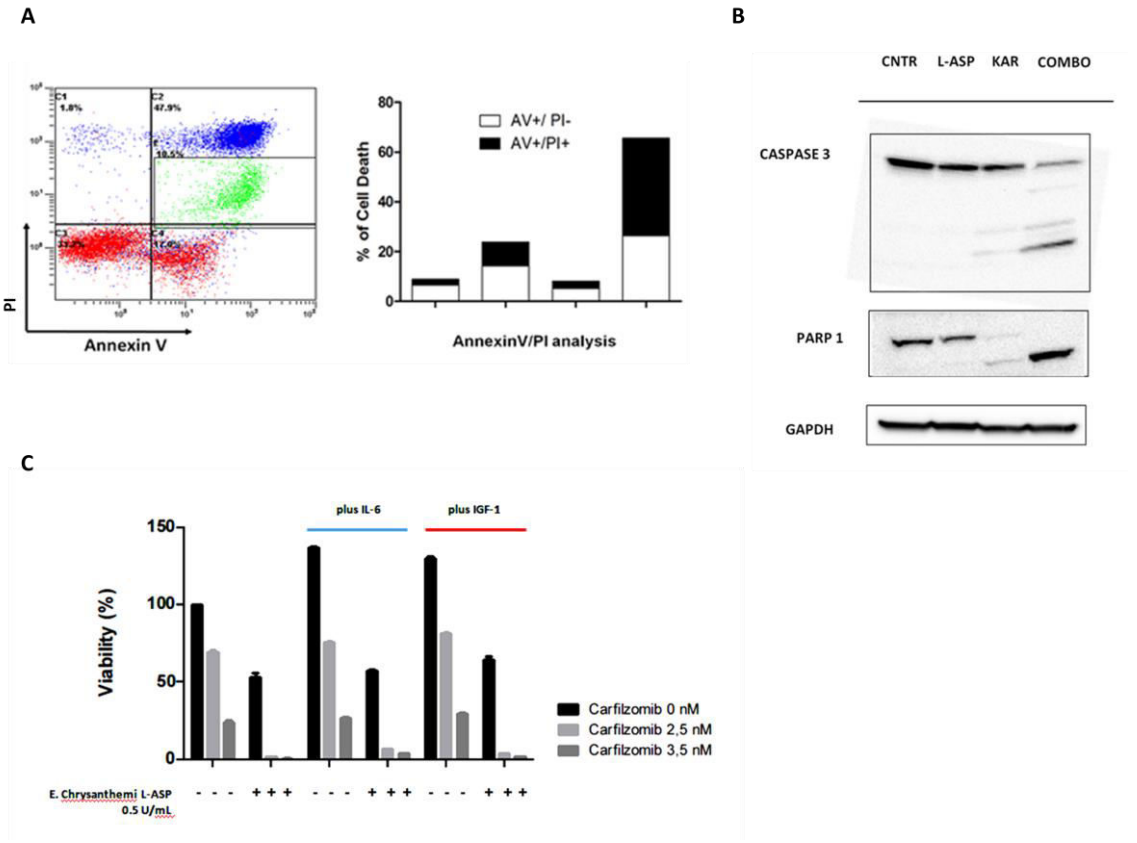

Figure 3. L-ASP induces synergistic growth inhibitory effects in combination with carfilzomib regardless of protective role of BM microenvironment. **(A)** LP1 cells were treated with L-ASP [0.5 U/mL], Carfilzomib [2 nM] or their combination. The percentage of apoptotic cells was measured after 48 h treatment by FACS analysis following AV/PI staining. **(B)** Whole cell lysates from LP1cells treated with each drug and their combination were subjected to WB analysis and probed with indicated antibodies. GAPDH was used as loading control. **(C)** MM-1S cells were treated with L-ASP [0.5 U/mL], Carfilzomib [2.5-3.5 nM] and combination in the presence or absence of rhIL-6 [10 ng/mL] or rhIGF-1 [100 ng/mL] for 48 hours. Viability was assessed by a MTS based assay. The results presented are a mean SD of triplicate samples

Based on pivotal role played by *c-MYC* in the anti-MM activity of L-ASP, we next investigated its modulation in such synergism. As shown in **Figure 4B** co-treatment induced massive *c-MYC* down-regulation corroborating its role also in this setting.

However, *c-MYC* negative U266 cells did not show weaker sensitivity, thus suggesting triviality of this oncogene in observed synergism (**Figure 4A and B**).

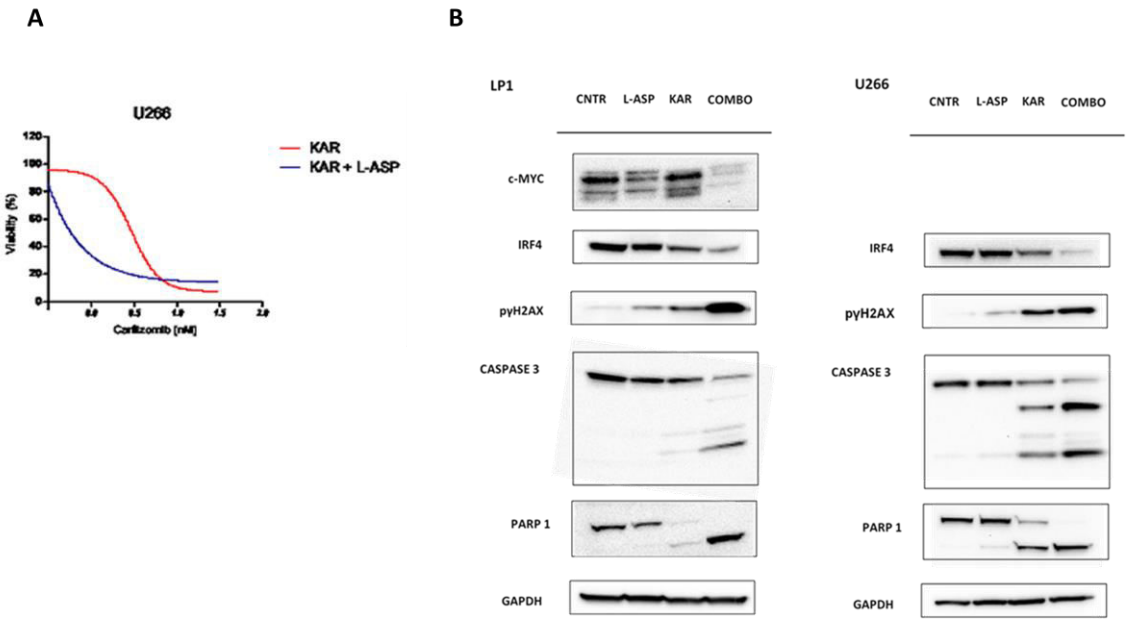

Figure 4. Cellular events triggered by drugs co-treatment. (A) U266 (Myc negative cells) were treated with increasing doses of L-ASP and PI combination. Viability was assessed by MTS-based assay. (**B**) Whole cell lysates from MM1S cells treated with several each drug and their combination, were subjected to WB analysis and probed with indicated antibodies. GAPDH was used as loading control.

To further support these results, we generated a stable *c-MYC* over-expressing U266 line by employing a lentiviral transduction approach (U266-cMYC OE). As shown in **Figure 5A**, engineered MM cells exhibited higher L-ASP sensitivity but slight-carfilzomib resistance; as result L-ASP plus carfilzomib showed comparable efficacy on both control and cMYC-OE U266cells. Remarkably, similar results were achieved by using different approaches: MTS based assay and PI-based FACS analysis (**Figure 5B and C**).

A

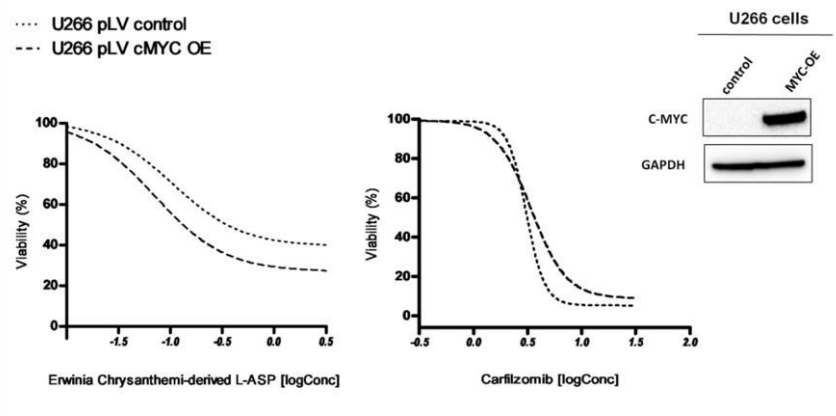

B

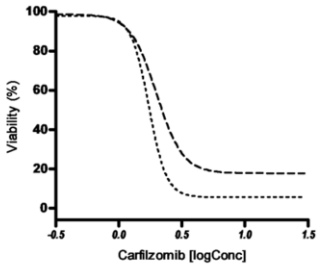

	U266 pLV control	U266 pLV cMYC OE
Erwinia Chrisanthemy-derived L-ASP IC50	0.1 U/mL	0.07 U/mL
Carfilzomib IC50	2.98 nM	3.40 nM
Combination IC50 [carfilzomib]	1.72 nM	1.88 nM

C

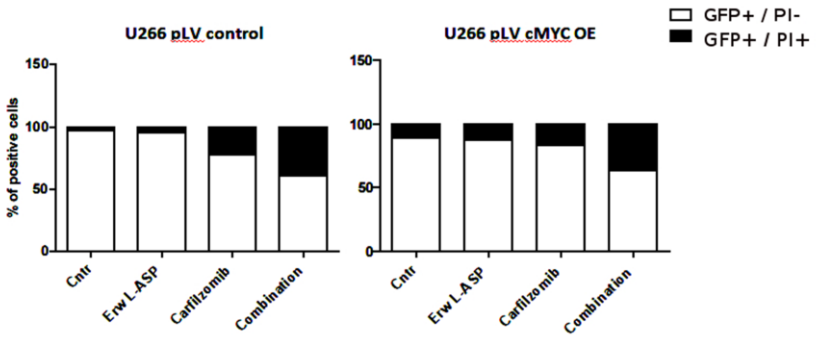

Figure 5. MYC is not crucial for anti-MM activity of observed synergism. (**A**) L-ASP and Carfilzomib alone were tested on U266 engineered cells. Control (dot line) and c-MYC-OE cells (dash line) were treated with increasing doses of drugs and viability was measured after 48h by using an MTS based-assay. (**B**) The anti-MM activity effectiveness of drugs combination was measured on both U266 cell lines (control and c-MYC-OE). (**C**) After 48h, cells viability was measured with FACS analysis after PI staining.

3.3 Role of metabolic shortage in modulating response to carfilzomib in MM cells

Next we investigated whether L-ASP and PI combination could affect MM cells viability due to impairment of metabolic processes. To gain insights into this phenomenon, we focused on intracellular levels of NAD+, a metabolite involved in maintenance of the mitochondrial membrane potential and cellular signaling.[41-43] As shown in **Figure 6A**, combination effectively reduced intracellular NAD+ concentration in MM cells, whereas the single agents treatment failed to diminish intracellular NAD+ content. Therefore, these results are consistent with a deep *metabolic shortage* triggered by co-treatment on MM cells. To investigate if intracellular NAD+ depletion could explain the synergism of L-ASP and PI combination, single drugs and their combination were tested in standard culture conditions and in presence of 1mM NAD or 10 mM nichotinamide (NAM) and 10 uM nicotinic acid. The percentage of apoptotic cells was evaluated by cytofluorimetric analysis after AV/PI staining. Interestingly, the addition of NAD or its precursors to culture medium was not able to revert the efficacy of the combination (data not shown).

The mitochondrial membrane potential ($\Delta\Psi m$) is an essential component in the process of energy storage during oxidative Phosphorylation and it is tightly interlinked to many mitochondrial processes, including ATP synthesis and ROS. By using tetramethylrhodamine ethyl ester (TMRE) cell staining, we found that single agents treatment did not induce mitochondrial transmembrane potential ($\Psi\Delta_m$) dissipation in MM cells, whilst their combination strongly enhanced this effect. (**Figure 6B**)

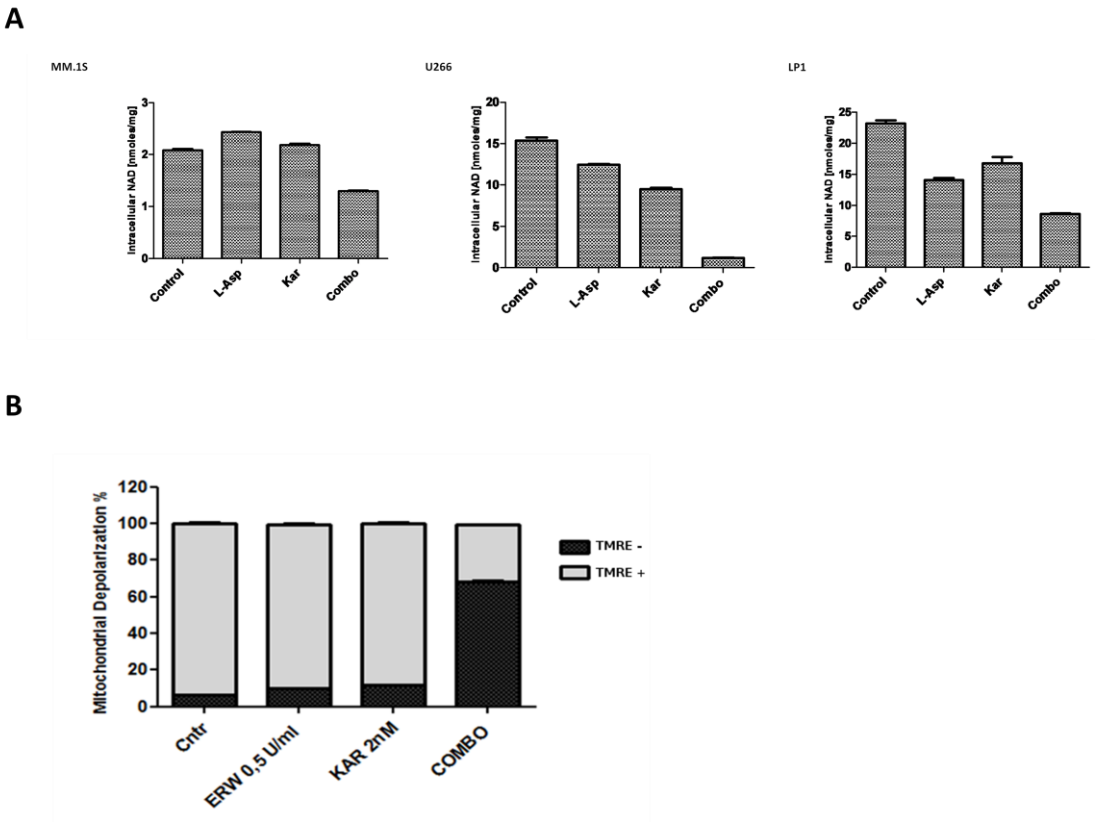

Figure 6. L-ASP plus carfilzomib induces potent anti-MM activity by triggering genotoxic stress. A) Intracellular NAD $^{+}$ concentration was measured in MM.1S, U266 and LP1 cell lines after 24 h of L-ASP, carfilzomib or their combination. Cells were plated at a density of 10^6 cells/well in 12-well plates. NAD+ values were normalized to protein concentrations, determined by Bradford assay. **B)** U266 cells were treated with single drugs and their combination for 48 h. Thereafter MM cells PBLs with conserved $\Psi\Delta_m$-high were quantified by flow-cytometry.

3.4 Combined L-ASP and carfilzomib increases genomic instability and oxidative stress of MM cells

Emerging data support existence of links between cancer metabolism and DNA damage, yielding opportunities to investigate these vulnerabilities in a wide range of tumors.[44,45] To determine the impact of L-ASP plus carfilzomib combination on genomic integrity of MM cells, we first asked whether such treatment leads to

accumulation of DNA damage by monitoring DNA damage signaling activity following single agents or their combinations. Co-treatment markedly increased the accumulation of the lower-molecular-weight protein γH2AX than specific controls. Similarly, L-ASP and carfilzomib co-treatment improvedγH2AX cellular foci compared with single agents treatment (**Figure 7A, B and C**). Collectively these data suggest that amino-acids starvation makes MM cells more vulnerable to carfilzomib activity probably through impairment of DNA repairs mechanisms efficiency, which in turn results in higher degree of DNA damage.

It has been previously reported that enhanced oxidative stress results in increased DNA damage observed in tumor cells.[45.47] As result, novel compounds have recently been described that exploit induction of ROS for treatment of cancer.[48] As a result we assumed that increased ROS levels promote DNA damage and induce apoptosis in MM co-treated cells. To formally demonstrate this hypothesis, we pre-treated MM cells with an antioxidant reagent N-Acetyl-Lcysteine (NAC), which scavenges ROS by replenishing glutathione stores. As shown in **Figure 7D**, this approach resulted in a complete rescue in term of both viability and apoptotic features of MM exposed cells, and more importantly, such treatment resulted in improved DNA stability, as suggested by reduced γ-H2A.X levels compared with control. (**Figure 7E**). Altogether, these data demonstrate that co-treatment elicits DNA damage in MM cells by both inducing oxidative stress and impairing DNA repair mechanisms efficiency.

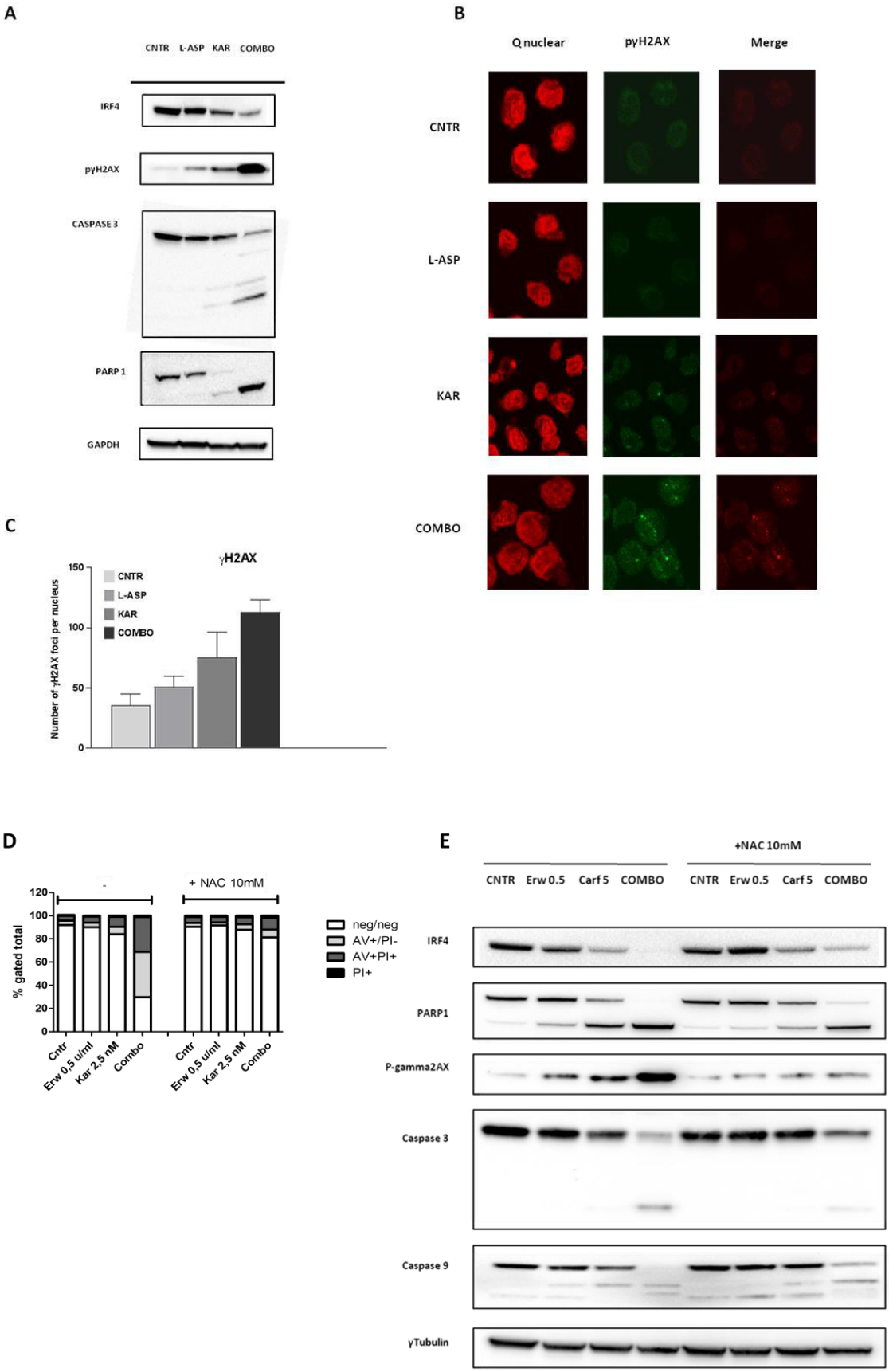
A
CNTR L-ASP KAR COMBO
IRF4
pγH2AX
CASPASE 3
PARP 1
GAPDH
B
Q nuclear
pγH2AX
Merge
CNTR
L-ASP
KAR
COMBO
C
γH2AX
Number of γH2AX foci per nucleus
150
100
50
0
CNTR
L-ASP
KAR
COMBO
D
% gated total
120
100
80
60
40
20
0
-
+ NAC 10mM
Cntr
Erw 0,5 u/ml
Kar 2,5 nM
Combo
neg/neg
AV+/PI-
AV+PI+
PI+
E
+NAC 10mM
CNTR Erw 0.5 Carf 5 COMBO
CNTR Erw 0.5 Carf 5 COMBO
IRF4
PARP1
P-gamma2AX
Caspase 3
Caspase 9
γTubulin

Figure 7. Whole cells lysate of MM treated cells were (**A**) subjected to western blot analysis or (**B**) fixed for immunofluorescence with γH2AX antibody and QNuclear. Scale bar 100 μm. (**C**) Data represent mean ± SD of 4 independent cell cultures, *** $P < 0.001$, shown is the percentage of cells showing >10 foci. (**D**) Single agents and their combination were tested in U266 cell line with or without 10mM of NAC for 48 hours. Apoptotic cells rate was assessed by FACS analysis after AV/PI staining. (**E**) Whole cells lysate of MM treated cells were subjected to western blot analysis in absence or in presence of 10mMol NAC for 24 hours.

4. DISCUSSION

Despite the dramatic improvements in MM treatment achieved in the last decade, it is still an incurable disease. MM is scarcely responsive to conventional chemotherapies and median overall survival was approximately 3 years until the late 1990s.[1] A better knowledge of the biological mechanisms involved in disease occurrence and progression has led to the development of several new, innovative, drugs that significantly improved patients outcome and renewed the therapeutic approach to the disease in the last years. At least 3 classes of agents targeting different biological mechanisms have become available: proteasome inhibitors, immunomodulatory agents, and monoclonal antibodies and have been incorporated into front-line treatment or in the relapsed/refractory setting.[4-6] Moreover, despite the improvement of patient risk-stratification systems at diagnosis, treatment outcome is often unpredictable due to the high degree of genomic heterogeneity and genomic instability which characterize the disease.[3] In this view, novel therapeutic strategies capable to overcome disease heterogeneity and improve patient outcome are strongly needed.

As well as most tumors, MM cells reprogram their metabolism to sustain uncontrolled proliferation and survival and several tumor-associated signaling pathways play a key-role in regulating metabolic processes in neoplastic cells.[9-13] The oncogenic role of *c-MYC* is well established in MM where it contributes to the malignant phenotype and disease progression.[49] Interestingly it has been reported that in neuroblastoma cells the oncogene *MYC* drives a transcriptional program that reprograms tumor

mitochondrial metabolism on Gln catabolism, to sustain cellular viability and TCA cycle anaplerosis.[50]

Moving from recent observations that MM cells are highly reliant on Gln for metabolic processes[22-24] we investigated the therapeutic relevance of Asparaginase-induced Gln depletion for MM treatment.[25-29] Pioneering studies on pediatric acute lymphoblastic leukemia patients explored the inter-relationship between asparaginase activity, Asn and Gln deamination. Gln deamination is significantly associated with clinically attainable plasmatic L-ASP activity and it is required for optimal serum Asn deamination, enhancing L-ASP efficacy in ALL patients. In fact, ≥ 90% of Gln deamination must occur before optimal Asn deamination takes place, due to *de novo* Asn synthesis in the liver.[51]

We observed that L-ASP treatment induces an early "metabolic shutdown" in HMCLs and MM primary cells as confirmed by cell cycle arrest in G1 phase and protein synthesis blockade in western blot analysis. Amino-acidic deprivation however does not result in direct citotoxicity in most of tested cell lines and several days are needed to induce cell death via apoptosis. We observed that following L-ASP treatment, *c-MYC* downregulation impaired cell cycle progression by CDK4 and CDK6 downregulation and loss of inhibition of p21 transcription. Notably, U266 cell line showed the highest IC50 value and did not show any modification of cell cycle progression under L-ASP treatment. A massive c-MYC downregulation was also observed in MM cells receiving L-ASP and PIs combination, suggesting a strong contribution of *c-MYC* downregulation driving the effectiveness of the combination, as already reported with Glutaminase-inhibitor compound 968 and carfilzomib association.[36] However, we confirmed the

effectiveness of L-ASP and PIs combination also in c-MYC negative U266 cell line, suggesting that the downregulation of the oncogene was not the main driver of the observed synergism.

Moving forward we explored whether the effectiveness of the combination could be explained by the impairment of metabolic cellular processes and oxidative stress induction. Normal plasma cells synthesize and secrete antibodies, being highly reliant on proteasome function for the clearance of abnormal and mutated proteins and on the "unfolded protein response" (UPR) signaling pathways. Malignant plasma cells transformation results in higher protein synthesis rates which makes cells more dependent on UPR signaling and proteasome functions for the clearance of abnormal proteins and proteins in excess. The pharmacological inhibition of proteasome function results in the accumulation of unfolded proteins triggering endoplasmic reticulum (ER) stress, which has until recently been considered the major mediator of PIs citotoxicity.[52,53] Unresolved ER stress is also responsible of reactive oxygen species (ROS) overproduction leading to oxidative stress in MM cells. Furthermore, recent reports disclosed the ability of PIs to directly induce oxidative stress in MM and other human cancer cells, underlying the importance of such mechanism in PIs citotoxicity.[55-57] We found that amino-acidic deprivation induced by L-ASP and PI co-treatment was able to induce loss of $\Delta\Psi m$ in comparison to single treatment alone, suggesting oxidative stress-induction as the main driver of L-ASP and PIs synergism. As a result we hypothesized that increased ROS levels promote DNA damage and induce apoptosis in MM co-treated cells. To formally demonstrate this hypothesis, we pre-treated MM cells with an antioxidant reagent NAC, which scavenges ROS by replenishing

glutathione stores. This approach resulted in a complete rescue in term of both viability and apoptotic features of MM exposed cells, and more importantly, such treatment resulted in improved DNA stability, Altogether, these data demonstrate that co-treatment elicits DNA damage in MM cells.

REFERENCES

1. Palumbo A, Anderson K. Multiple myeloma. N Engl J Med. 2011 Mar 17;364(11):1046-60.
2. Rajkumar SV, Kumar S. Multiple Myeloma: Diagnosis and Treatment. Mayo Clin Proc. 2016 Jan;91(1):101-19.
3. Ludwig H, Miguel JS, Dimopoulos MA, et al. International Myeloma Working Group recommendations for global myeloma care. Leukemia. 2014 May;28(5):981-92.
4. Kumar SK, Callander NS, Alsina M, et al. NCCN Guidelines Insights: Multiple Myeloma, Version 3.2018. J Natl Compr Canc Netw. 2018 Jan;16(1):11-20.
5. Guerrero-Garcia TA, Gandolfi S, Laubach JP, et al. The power of proteasome inhibition in multiple myeloma. Expert Rev Proteomics. 2018 Dec;15(12):1033-1052.
6. Herndon TM, Deisseroth A, Kaminskas E, et al. U.s. Food and Drug Administration approval: carfilzomib for the treatment of multiple myeloma. Clin Cancer Res. 2013 Sep 1;19(17):4559-63.
7. Garderet L, Laubach JP, Stoppa AM, et al. Association between response kinetics and outcomes in relapsed/refractory multiple myeloma: analysis from TOURMALINE-MM1. Leukemia. 2018 Sep;32(9):2032-2036.
8. Leung-Hagesteijn C, Erdmann N, Cheung G, et al. Xbp1s-negative tumor B cells and pre-plasmablasts mediate therapeutic proteasome inhibitor resistance in multiple myeloma. Cancer Cell. 2013 Sep 9;24(3):289-304.

9. Pavlova NN, Thompson CB. The Emerging Hallmarks of Cancer Metabolism. Cell Metab. 2016 Jan 12;23(1):27-47.
10. DeBerardinis RJ, Lum JJ, Hatzivassiliou G, Thompson CB. The biology of cancer: metabolic reprogramming fuels cell growth and proliferation. Cell Metab. 2008 Jan;7(1):11-20.
11. Vander Heiden MG, Cantley LC, Thompson CB. Understanding the Warburg effect: the metabolic requirements of cell proliferation. Science. 2009 May 22;324(5930):1029-33.
12. Maria V. Liberti and Jason W. Locasale. The Warburg Effect: How Does it Benefit Cancer Cells? Trends Biochem Sci. 2016 Mar; 41(3): 211–218.
13. Shanware NP, Mullen AR, DeBerardinis RJ, Abraham RT. Glutamine: pleiotropic roles in tumor growth and stress resistance. JMol Med (Berl). 2011 Mar;89(3):229-36.
14. Wise DR, Thompson CB. Glutamine addiction: a new therapeutic target in cancer. Trends Biochem Sci. 2010 Aug;35(8):427-33.
15. Altman B, Stine Z, Dang CV. From Krebs to clinic: glutamine metabolism to cancer therapy. Nat Rev Cancer. 2016 Oct;16(10):619-34.
16. Le A, Lane AN, Hamaker M, et al. Glucose-independent glutamine metabolism via TCA cycling for proliferation and survival in B cells. Cell Metab. 2012 Jan 4;15(1):110-21.
17. Cory JG and Cory AH. Critical roles of glutamine as nitrogen donors in purine and pyrimidine nucleotide synthesis: asparaginase treatment in childhood acute lymphoblastic leukemia. In Vivo. 2006 Sep-Oct;20(5):587-9.

18. Sappington DR, Siegel ER, Hiatt G, et al. Glutamine drives glutathione synthesis and contributes to radiation sensitivity of A549 and H460 lung cancer cell lines. Biochim Biophys Acta. 2016 Apr;1860(4):836-43.
19. Zhan H, Ciano K, Dong K and Zucker S. Targeting glutamine metabolism in myeloproliferative neoplasms. Blood Cells Mol Dis. 2015 Oct; 55(3): 241–247.
20. Xiang Y, Stine ZE, Xia J, et al. Targeted inhibition of tumor-specific glutaminase diminishes cell-autonomous tumorigenesis. J Clin Invest. 2015 Jun;125(6):2293-306.
21. Korangath P, Teo WW, Sadik H, et al. Targeting Glutamine Metabolism in Breast Cancer with Aminooxyacetate. Clin Cancer Res. 2015 Jul 15;21(14):3263-73.
22. Bolzoni M, Chiu M, Accardi F, et al. Dependence on glutamine uptake and glutamine addiction characterize myeloma cells: a new attractive target. Blood. 2016 Aug 4;128(5):667-79.
23. Giuliani N, Chiu M, Bolzoni M, et al. The potential of inhibiting glutamine uptake as a therapeutic target for multiple myeloma. Expert OpinTher Targets. 2017 Mar;21(3):231-234.
24. Effenberger M, Bommert KS, Kunz V, et al. Glutaminase inhibition in multiple myeloma induces apoptosis via MYC degradation. Oncotarget. 2017 Aug 24;8(49):85858-85867.
25. Covini D, Tardito S, Bussolati O, et al. Expanding targets for a metabolic therapy of cancer: L-asparaginase. Recent Pat Anticancer Drug Discov. 2012 Jan;7(1):4-13.

26. Avramis VI, Panosyan EH.Pharmacokinetic/pharmacodynamic relationships of asparaginase formulations: the past, the present and recommendations for the future.ClinPharmacokinet. 2005;44(4):367-93
27. Sugimoto K, Suzuki HI, Fujimura T, et al. A clinically attainable dose of L-asparaginase targets glutamine addiction in lymphoid cell lines.Cancer Sci. 2015 Nov;106(11):1534-43.
28. Purwaha P, Lorenzi PL, Silva LP, Hawke DH, Weinstein JN. Targeted metabolomic analysis of amino acid response to L-asparaginase in adherent cells.Metabolomics. 2014;10(5):909-919. Epub 2014 Feb 7.
29. Reinert RB, Oberle LM, Wek SA, et al. Role of glutamine depletion in directing tissue-specific nutrient stress responses to L-asparaginase. JBiol Chem. 2006 Oct 20;281(42):31222-33. Epub 2006 Aug 24.
30. Bruzzone S, De Flora A, Usai C, Graeff R, Lee HC. Cyclic ADP-ribose is a second messenger in the lipopolysaccharide-stimulated proliferation of human peripheral blood mononuclear cells.Biochem J. 2003 Oct 15;375(Pt 2):395-403.
31. Piacente F, Caffa I, Ravera S, et al. Nicotinic Acid Phosphoribosyltransferase Regulates Cancer Cell Metabolism, Susceptibility to NAMPT Inhibitors, and DNA Repair. Cancer Res. 2017 Jul 15;77(14):3857-3869..
32. Chiu M, Tardito S, Pillozzi S, et al. Glutamine depletion by crisantaspase hinders the growth of human hepatocellular carcinoma xenografts. Br J Cancer. 2014 Sep 9;111(6):1159-67.

33. Karpel-Massler G, Ramani D, Shu C, et al. Metabolic reprogramming of glioblastoma cells by L-asparaginase sensitizes for apoptosis in vitro and in vivo. Oncotarget. 2016 Jun 7;7(23):33512-28.

34. Bergaggio E, Riganti C, Garaffo G, et al. IDH2 inhibition enhances proteasome inhibitor responsiveness in hematological malignancies. Blood. 2019 Jan 10;133(2):156-167.

35. Cagnetta A, Cea M, Calimeri T, et al. Intracellular NAD^+ depletion enhances bortezomib-induced anti-myeloma activity. Blood. 2013 Aug 15;122(7):1243-55.

36. Thompson RM, Dytfeld D, Reyes L, et al. Glutaminase inhibitor CB-839 synergizes with carfilzomib in resistant multiple myeloma cells.Oncotarget. 2017 May 30;8(22):35863-35876.

37. Hideshima T, Richardson P, Chauhan D, Palombella VJ, Elliott PJ, Adams J, Anderson KC. The proteasome inhibitor PS-341 inhibits growth, induces apoptosis, and overcomes drug resistance in human multiple myeloma cells. Cancer Res. 2001 Apr 1;61(7):3071-6.

38. Cea M, Cagnetta A, Fulciniti M, et al. Targeting NAD+ salvage pathway induces autophagy in multiple myeloma cells via mTORC1 and extracellular signal-regulated kinase (ERK1/2) inhibition. Blood. 2012 Oct 25; 120(17): 3519–3529.

39. Hideshima T, Mitsiades C, Tonon G, Richardson PG, Anderson KC. Understanding multiple myeloma pathogenesis in the bone marrow to identify new therapeutic targets. Nat Rev Cancer. 2007 Aug;7(8):585-98.

40. McMillin DW, Delmore J, Weisberg E, et al. Tumor cell-specific bioluminescence platform to identify stroma-induced changes to anticancer drug activity. Nat Med. 2010 Apr;16(4):483-9.
41. Berger F, Ramírez-Hernández MH, Ziegler M. The new life of a centenarian: signalling functions of NAD(P). Trends Biochem Sci. 2004 Mar;29(3):111-8.
42. Chiarugi A, Dölle C, Felici R, Ziegler M. The NAD metabolome--a key determinant of cancer cell biology. Nat Rev Cancer. 2012 Nov;12(11):741-52.
43. Shackelford RE, Mayhall K, Maxwell NM, Kandil E, Coppola D. Nicotinamide phosphoribosyltransferase in malignancy: a review. Genes Cancer. 2013 Nov;4(11-12):447-56.
44. Kryston TB, Georgiev AB, Pissis P, Georgakilas AG. Role of oxidative stress and DNA damage in human carcinogenesis. Mutat Res. 2011 Jun 3;711(1-2):193-201.
45. Tran TQ, Ishak Gabra MB, Lowman XH. Glutamine deficiency induces DNA alkylation damage and sensitizes cancer cells to alkylating agents through inhibition of ALKBH enzymes. PLoS Biol. 2017 Nov 6;15(11):e2002810.
46. Bartkova J, Horejsí Z, Koed K, et al. DNA damage response as a candidate anti-cancer barrier in early human tumorigenesis. Nature. 2005 Apr 14;434(7035):864-70
47. Cottini F, Hideshima T, Suzuki R, et al. Synthetic Lethal Approaches Exploiting DNA Damage in Aggressive Myeloma. Cancer Discov. 2015 Sep;5(9):972-87.
48. Trachootham D, Zhou Y, Zhang H, et al. Selective killing of oncogenically transformed cells through a ROS-mediated mechanism by beta-phenylethyl isothiocyanate. Cancer Cell. 2006 Sep;10(3):241-52.

49. Chng WJ, Huang GF, Chung TH, et al. Clinical and biological implications of MYC activation: a common difference between MGUS and newly diagnosed multiple myeloma. Leukemia. 2011 Jun;25(6):1026-35.
50. Wise DR, DeBerardinis RJ, Mancuso A, et al. Myc regulates a transcriptional program that stimulates mitochondrial glutaminolysis and leads to glutamine addiction. Proc Natl Acad Sci U S A. 2008 Dec 2;105(48):18782-7.
51. Grigoryan RS, Panosyan EH, Seibel NL, Gaynon PS, Avramis IA, Avramis VI.Changes of amino acid serum levels in pediatric patients with higher-risk acute lymphoblastic leukemia (CCG-1961). In Vivo. 2004 Mar-Apr;18(2):107-12.
52. Obeng EA, Carlson LM, Gutman DM, Harrington WJ Jr, Lee KP, Boise LH.et al. Proteasome inhibitors induce a terminal unfolded protein response in multiple myeloma cells. Blood. 2006 Jun 15;107(12):4907-16. Epub 2006 Feb 28.
53. Lee AH, Iwakoshi NN, Anderson KC, Glimcher LH. Proteasome inhibitors disrupt the unfolded protein response in myeloma cells. Proc Natl Acad Sci U S A. 2003 Aug 19;100(17):9946-51.
54. Lipchick BC, Fink EE, Nikiforov MA. Oxidative stress and proteasome inhibitors in multiple myeloma. Pharmacol Res. 2016 Mar;105:210-5.
55. Weniger MA, Rizzatti EG, Pérez-Galán P, et al. Treatment-induced oxidative stress and cellular antioxidant capacity determine response to bortezomib in mantle cell lymphoma. Clin Cancer Res. 2011 Aug 1;17(15):5101-12.
56. Starheim K, Holien T, Misund K, et al. Intracellular glutathione determines bortezomib cytotoxicity in multiple myeloma cells. Blood Cancer J. 2016 Jul; 6(7): e446.

57. Nerini-Molteni S, Ferrarini M, Cozza S, Caligaris-Cappio F, Sitia R. Redox homeostasis modulates the sensitivity of myeloma cells to bortezomib. Br J Haematol. 2008 May;141(4):494-503.